PHYSICAL REVIEW B VOLUME 46, NUMBER 16 15 OCTOBER 1992-II

Interchain interactions in polyacetylene: Optical properties and photoconductive response

D. Comoretto, G. Dellepiane, and G. F. Musso
Istituto di Chimica Industriale, Università di Genova, Corso Europa, 30-16132 Genova, Italy

R. Tubino
Istituto di Matematica e Fisica, Università di Sassari, via Vienna, 2-07100 Sassari, Italy

R. Dorsinville, A. Walser, and R. R. Alfano
Institute for Ultrafast Laser Spectroscopy, The City College of New York, 138th and Convent Avenue, New York, New York 10031
and Electrical Engineering Department, The City College of New York,
138th and Convent Avenue, New York, New York 10031

(Received 3 June 1992)

A simple tight-binding model extended to include the zig-zag structure of the chains and the interchain electronic coupling has been used to account for the dispersion of the real and imaginary part of the dielectric function of polyacetylene as derived from optical measurements. The model also accounts for the pump polarization anisotropy observed in the photoexcitation of oriented *trans*-$(CH)_x$. It is established that a relatively small hopping integral ($\beta_\perp \simeq 0.05$ eV), combined with laser heating effects, accounts for the observed experimental features, assuming that bimolecular recombination does not occur.

I. INTRODUCTION

Experiments on the photoconductivity and on the photoinduced absorption carried out both on fibrous[1] and Durham[2,3] highly oriented *trans*-polyacetylene have revealed an intriguing aspect of the carrier photogeneration in one-dimensional semiconductors. Figure 1 shows the picosecond photocurrent as a function of the angle formed between the electrical vector of the exciting radiation and the chain direction. These data, relative to fibrous polyacetylene stretched up to seven times, show that the response is maximum when the exciting radiation is polarized perpendicularly to the chain direction. Various experimental findings concerning the anisotropy of the photoresponse with respect to the "pump" polarization can be summarized as follows.

(i) The anisotropy of the photoconductive (PC) response is comparable with that of the photoinduced "midgap"[1,2] absorption, thus showing that this kind of anisotropy is related to photogeneration of the carrier rather than to their mobility.

(ii) After correcting for the reflectivity anisotropy the subgap (1.17-eV) photocurrent exhibits a pump anisotropy smaller ($\simeq 2$) than the photocurrent anisotropy (4–8) resulting from visible excitation (2.34 eV). Moreover, the latter strongly decreases as the laser intensity is increased[4] (Fig. 2).

(iii) A pump anisotropy is observed both for cw and pulsed (25-ps) excitation.[2,4]

There are, in principle, two possible explanations for this effect. One proposed by Blanchet *et al.*[5] and Dorsinville *et al.*[1] is related to a bimolecular recombination of the carriers and can be traced back to the topological nature of the soliton excitations. This model, which has been discussed in detail in a previous publication,[1] has been questioned by Bleier *et al.*[3] who have shown that, at least for Durham polyacetylene, the rate of decay of the slow PC component is intensity independent.

The other explanation, proposed by Townsend and Friend,[2] is related to the direct interchain carrier photogeneration, whose rate is maximum for perpendicular excitations. This model requires a small but nonvanishing perpendicular absorption. Unfortunately the direct experimental observation of this interchain perpendicular absorption is hampered by two factors: the intrachain perpendicular absorption due to the zig-zag structure of the chain and the perpendicular absorption due to chain misalignment. The latter component is given by $\alpha_\parallel \sec^2(\delta)$, for a tilt angle δ. The chain misalignment depends on the morphology of the sample, fibrillar $(CH)_x$ showing an anisotropy $\alpha_\parallel/\alpha_\perp \simeq 15$ (Ref. 6) while Durham $(CH)_x$ shows an anisotropy of $\simeq 25$.[2,7]

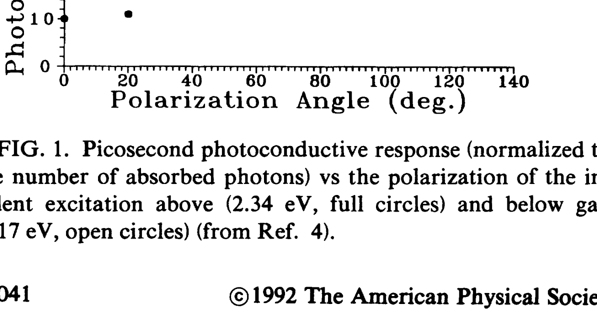

FIG. 1. Picosecond photoconductive response (normalized to the number of absorbed photons) vs the polarization of the incident excitation above (2.34 eV, full circles) and below gap (1.17 eV, open circles) (from Ref. 4).

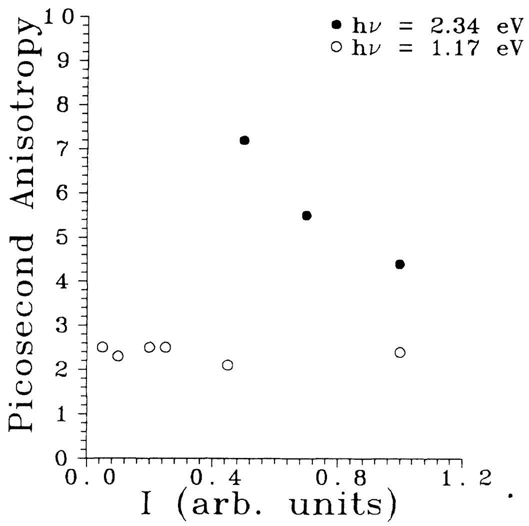

FIG. 2. Intensity dependence of the ps pump anisotropy of the photocurrent. Each curve has been normalized to the number of the absorbed photons (see Ref. 4). Full circles, excitations at 2.34 eV; open circles, excitation at 1.17 eV.

The effect of direct interchain carrier photogeneration on the pump anisotropy depends on two characteristic times: the self-trapping time in a one-dimensional lattice ($\tau_{1D} \simeq 1/\omega_{ph}$, $\hbar\omega_{ph}$ being the average phonon energy) and the time needed for the carriers to hop to a different chain ($\tau_\perp \simeq \hbar/\beta_\perp$). These times control the fraction of carriers escaping the geminate recombination $\xi \simeq (\tau_{1D}/\tau_\perp)^2$. Two limiting cases can occur.

(1) $\tau_{1D} \ll \tau_\perp$ ($\beta_\perp \ll \hbar\omega_{ph}$); in this case the electron-hole (*e-h*) pair is quickly trapped on the same chain and disappears through geminate recombination, and only a small fraction of photogenerated carriers manages to separate on different chains. In this case the direct *e-h* separation produced by a perpendicular interchain absorption coefficient produces a large pump anisotropy.

(2) If, on the other hand, $\tau_{1D} \gg \tau_\perp$ ($\beta_\perp \gg \hbar\omega_{ph}$), many carriers will be able to hop on different chains before relaxing into solitons. In this case the effect of the perpendicular interchain absorption will be negligible. Since estimated values for $\beta_\perp$ range in 0.01–0.1 eV,[8,9] and a typical C=C stretching energy is about 0.15 eV, *trans*-$(CH)_x$ falls into the intermediate case ($\beta_\perp < \hbar\omega_{ph}$) and some pump anisotropy is therefore expected.

The aim of this paper is to evaluate the anisotropy of the photoconductive response with respect to the pump polarization in *trans*-$(CH)_x$ by working out a simple band-structure model to compute the anisotropy and the dispersion of the dielectric function of this polymer. A number of papers have already appeared on this matter.[8,10–16] We will present here a relatively simplified model for the interchain interactions that has the advantage of providing simple analytical expressions for the dipole moment components as a function of only one interchain parameter ($\beta_\perp$), therefore providing a simple semiquantitative picture of the basic physics of the interchain coupling.

II. THEORETICAL MODEL

As already discussed, we assume that the self-trapping of the photogenerated *e-h* pair into an $S^+\bar{S}^-$ pair is faster than the interchain charge separation (nonadiabatic photogeneration). As a consequence, a fraction $\xi \simeq (\tau_{1D}/\tau_\perp)^2$ of the intrachain carriers will manage to transfer on different chains.[13,17] It is safe to assume that only carriers which have managed to separate on different chains and carriers directly created by interchain absorption can contribute to the overall photoconductive response, while pairs on the same chain or segment undergo a quick one-dimensional recombination. If this is the case, the concentration of long-lived carriers created with the polarization parallel ($n_\parallel$) and perpendicular ($n_\perp$) to the chain on a plane at distance x from the illuminated surface is given by the following rate equations:

$$\frac{dn_\parallel(x)}{dt} = \eta\xi\alpha_\parallel I \exp(-\alpha_\parallel x) - \frac{n_\parallel(x)}{\tau} , \tag{1a}$$

$$\frac{dn_\perp(x)}{dt} = \eta\{\xi[\alpha_\parallel \sec^2(\delta) + \alpha_\perp^{1D}] + \alpha_\perp^{3D}\} \times I \exp(-\alpha_\perp x) - \frac{n_\perp(x)}{\tau} , \tag{1b}$$

where η is the probability that an impinging photon creates an *e-h* pair ($\eta \simeq 1$ for photon energies greater than the band gap E_g), ξ is the probability of escaping geminate recombination for intrachain carriers, $\alpha_\parallel$ is the absorption coefficient along the stretching direction, $\alpha_\perp^{1D}$ and $\alpha_\perp^{3D}$ are the perpendicular intrachain and interchain absorption coefficients, respectively, I is the number of photons per unit time per unit square area, $\alpha_\perp = \alpha_\parallel \sec^2(\delta) + \alpha_\perp^{1D} + \alpha_\perp^{3D}$ is the overall perpendicular absorption coefficient, and τ the monomolecular recombination time.

In Eq. (1a) the generation term corresponds to the creation of carriers following absorption of photons polarized along the chain axis. Carriers created by perpendicular polarization [Eq. (1b)] arise from three different generation processes: (i) The chain misorientation which gives rise to a perpendicular absorption coefficient $\alpha_\parallel \sec^2(\delta)$. (ii) The intrachain perpendicular absorption originating from the zig-zag structure of the single chain. (iii) Direct generation of carriers on different chains originating from finite transverse bandwidth.

Equations (1a) and (1b) can be integrated to yield the total numbers $N_\parallel$ and $N_\perp$ of long-lived carriers created with the two polarizations:

$$N_\parallel = \left[\frac{1}{d_\parallel} \int_0^\infty dx\, n_\parallel(x) \right] A d_\parallel = A\tau\eta\xi I , \tag{2a}$$

$$N_\perp = \left[\frac{1}{d_\perp} \int_0^\infty dx\, n_\perp(x) \right] A d_\perp = A\tau\eta \frac{I}{\alpha_\perp} \{\xi[\alpha_\parallel \sec^2(\delta) + \alpha_\perp^{1D}] + \alpha_\perp^{3D}\} , \tag{2b}$$

where $d_\parallel \simeq 1/\alpha_\parallel$ and $d_\perp \simeq 1/\alpha_\perp$ are the radiation penetra-

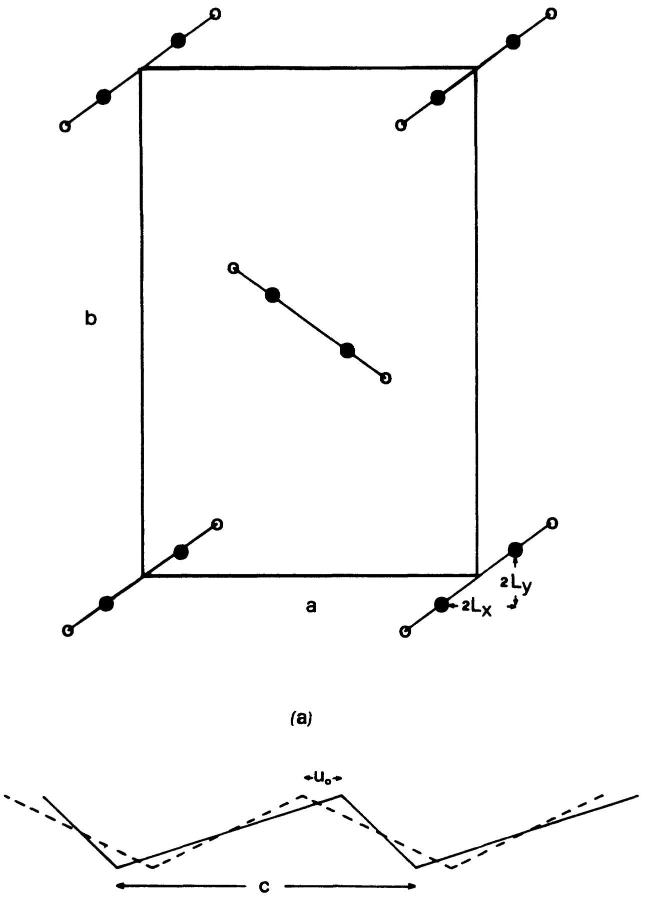

(a)

(b)

FIG. 3. (a) Sketch of the unit cell of *trans*-(CH)$_x$ in a plane perpendicular to the chain axis (full circles, carbon atoms; open circle, hydrogen atoms). $2L_x$ and $2L_y$ are the projections of the chain width on the crystallographic x and y axes, respectively. (b) Dimerized (full line) and undimerized (broken line) bonds in the chain plane. u_0 is the displacement of the carbon atoms due to the dimerization (see Ref. 24).

tion depths for the two polarizations and A is the illuminated area.

The carrier anisotropy is then given by

$$\frac{N_\perp}{N_\parallel}=1-\frac{\alpha_\perp^{3D}}{\alpha_\perp}\left[1-\frac{1}{\xi}\right]\simeq 1+\frac{\alpha_\perp^{3D}}{\alpha_\perp}\frac{1}{\xi} \tag{3}$$

being $\xi \ll 1$ as measured by Orenstein *et al.*[17] Since the measurement of the absorption coefficient with perpendicular polarization provides the value of $\alpha_\perp$, $\alpha_\perp^{3D}$ cannot be directly determined. In order to overcome this difficulty, we will attempt an evaluation of the absorption coefficients by working out a simple extension of the tight-binding model to include interchain interactions and the zig-zag structure of the chain.

The model adopted assumes planar zig-zag chains organized in the three-dimensional crystal structure[18] shown in Fig. 3. According to Refs. 19 and 20 the electronic transition moment is given by

$$\mathbf{M}_{ss'}(\mathbf{k})=\frac{i}{V}\int u_{s'\mathbf{k}}^{*}(\mathbf{r})\nabla_k u_{s\mathbf{k}}(\mathbf{r})d^3\mathbf{r} , \tag{4}$$

where $\mathbf{k}$ is the wave vector corresponding to the vertical optical transition, V is the volume of the unit cell, $d^3\mathbf{r}$ is the infinitesimal volume element, and $u_{s\mathbf{k}}$ is the unit-cell periodic part of the Bloch wave function $\Phi_{s\mathbf{k}}$,

$$\Phi_{s\mathbf{k}}(\mathbf{r})=e^{i\mathbf{k}\cdot\mathbf{r}}u_{s\mathbf{k}}(\mathbf{r}) . \tag{5}$$

In the crystal structure of *trans*-polyacetylene the unit cell contains two inequivalent chains. The wave function Φ is constructed as a linear combination of the atomic orbitals belonging to the two chains:

$$\Phi_{s\mathbf{k}}(\mathbf{r})=(N_1N_2N_3)^{-1/2}\times\sum_{l=1}^{N_1}\sum_{m=1}^{N_2}\sum_{n=1}^{N_3} e^{A(l,m,n)}B(l,m,n) , \tag{6a}$$

$$A(l,m,n)=i\mathbf{k}\cdot[(l-1)a\mathbf{e}_x+(m-1)b\mathbf{e}_y+(n-1)c\mathbf{e}_z] , \tag{6b}$$

$$B(l,m,n)=C_1^{s\mathbf{k}}\phi_{4l-3,4m-3,4n-3}+C_2^{s\mathbf{k}}\phi_{4l-2,4m-2,4n-2}+C_3^{s\mathbf{k}}\phi_{4l-1,4m-1,4n-1}+C_4^{s\mathbf{k}}\phi_{4l,4m,4n} , \tag{6c}$$

where the ϕ's are the atomic wave functions for the $2p\pi$ electrons, and the $C^{s\mathbf{k}}$ are the expansion coefficients which can be determined by minimizing the total π electronic energy of the crystal. By inserting Eqs. (6) into Eq. (4) and using the relation

$$\int \phi_i^* \mathbf{x}\phi_j d^3\mathbf{r}=\delta_{ij}\mathbf{x}_i \tag{7}$$

one obtains for the x component of the electronic transition moment

$$M_{ss'}^{x}(\mathbf{k})=\sum_{p=1}^{4}\left[C_p^{s'*}C_p^{s}x_p+iC_p^{s'*}\frac{\partial}{\partial k_x}C_p^{s}\right] , \tag{8}$$

with analogous expressions holding for the y and z components. Evaluation of (8) requires analytical expressions for the expansion coefficients. If the interactions within the cell are neglected and only the closest interactions between equivalent chains in the x direction are included,[6] the 4×4 equation splits into two identical 2×2 equations of the form

$$\begin{vmatrix} -\varepsilon & \beta_1+\beta_2\exp(-ik_zc)+\beta_\perp\exp(-ik_xa) \\ \beta_1+\beta_2\exp(ik_zc)+\beta_\perp\exp(ik_xa) & -\varepsilon \end{vmatrix}=0 , \tag{9}$$

where β_1 and β_2 indicate intrachain transfer integrals along the single and double bonds, respectively, and $\beta_\perp$ the interchain transfer integral. If we put $\beta = \beta_1 + \beta_2 \exp(-ik_z c) + \beta_\perp \exp(-ik_x a)$, the expansion coefficients are given by

$$C_1^v = C_1^c = 1/\sqrt{2}(\beta/\beta^*)^{1/4} , \tag{10a}$$

$$C_2^v = -C_2^c = -1/\sqrt{2}(\beta^*/\beta)^{1/4} \tag{10b}$$

and we obtain the following expressions for the components of the conduction-valence transition moment:

$$M_{cv}^x(\mathbf{k}) = \frac{a}{4\varepsilon^2}[\varepsilon^2 - \varepsilon_0^2 + \beta_\perp^2] - L_x , \tag{11a}$$

$$M_{cv}^y(\mathbf{k}) = -L_y , \tag{11b}$$

$$M_{cv}^z(\mathbf{k}) = -\left[u_0 + \frac{c}{4\varepsilon^2}[\varepsilon^2 - \varepsilon_0^2 - \beta_2^2 + \beta_1^2 \right. \\ \left. - 2\beta_2\beta_\perp \cos(k_z c - k_x a)] \right] . \tag{11c}$$

In (11) ε is the two-band solution of (9)

$$\varepsilon^2(\mathbf{k}) = \varepsilon_0^2(\mathbf{k}) + \beta_\perp^2 + 2\beta_1\beta_\perp \cos(k_x a) \\ + 2\beta_2\beta_\perp \cos(k_z c - k_x a) , \tag{12a}$$

$$\varepsilon_0^2(\mathbf{k}) = \beta_1^2 + \beta_2^2 + 2\beta_1\beta_2 \cos(k_z c) , \tag{12b}$$

where $\varepsilon_v = -\varepsilon_c$ and $\varepsilon_c = \varepsilon$, u_0 is the displacement parallel to the chain direction due to the dimerization [Fig. 3(b)] and $2L_x, 2L_y$ are the projections of the chain width on the crystallographic x and y axes, respectively [Fig. 3(a)]. We remark that the expressions (11) are slightly different from those previously published by us,[6,21,22] in which the effect of the dimerization and of the zig-zag structure of the chain were not considered, and a misprint [a factor of 2 in Eq. (11c)] occurred.

The interchain and intrachain components of the transition moments are then given by

$$\mathbf{M}_{cv}^\perp(\mathbf{k})_{\text{inter}} = \frac{a}{4\varepsilon^2}[\varepsilon^2 - \varepsilon_0^2 + \beta_\perp^2] , \tag{13}$$

$$\mathbf{M}_{cv}^\perp(\mathbf{k})_{\text{intra}} = c/(4\sqrt{3}) . \tag{14}$$

By putting $\beta_\perp = 0$ and using the relation between the $\hat{\mathbf{p}}$ and $\hat{\mathbf{x}}$ representation ($|\hat{\mathbf{p}}_{cv}|^2 = m^2(\hbar\omega)^2/\hbar^2 |\hat{\mathbf{x}}_{cv}|^2$) (Ref. 23) this model yields the expressions derived by Baeriswyl *et al.*[24] in the single chain approximation. From expressions (13) and (14) the optical response function can be evaluated using standard relations.[23]

III. OPTICAL PROPERTIES

In a conjugated polymer σ and π electrons give rise to energy bands well separated in energy. The localized σ electrons originate a weakly dispersed band possessing high excitation energy. On the other hand, the π electrons, which are delocalized over the whole chain, originate a band with considerable width ($\simeq 10$ eV). The electric susceptibility can then be written

$$\chi(\omega) = \chi_\sigma + \chi_\pi(\omega) , \tag{15}$$

where the contribution χ_σ coming from the σ electrons is evaluated within the framework of the bond polarizability theory[20,25,26] and can be considered independent on the energy $\hbar\omega$, and $\chi_\pi(\omega)$ is the contribution coming from the π electrons. For a stretch-oriented polymer Eq. (15) becomes

$$\chi^\parallel(\omega) = \chi_\sigma^\parallel + \chi_\pi^\parallel(\omega) , \tag{16a}$$

$$\chi^\perp(\omega) = \chi_\sigma^\perp + \chi_\pi^\perp(\omega) . \tag{16b}$$

Because of the local-field correction[20] the perpendicular component of the dielectric function $\varepsilon(\omega)$ is related to $\chi(\omega)$ by

$$\varepsilon^\perp(\omega) = \frac{1 + 2\pi\chi^\perp(\omega)}{1 - 2\pi\chi^\perp(\omega)} , \tag{17a}$$

whereas the parallel component is

$$\varepsilon^\parallel(\omega) = 1 + 4\pi\chi^\parallel(\omega) . \tag{17b}$$

Standard relations are used to calculate the absorption coefficient (α) and the reflectivity (R)

$$n(\omega) = \tfrac{1}{2}\{[\varepsilon_1^2(\omega) + \varepsilon_2^2(\omega)]^{1/2} + \varepsilon_1(\omega)\}^{1/2} , \tag{18a}$$

$$k(\omega) = \tfrac{1}{2}\{[\varepsilon_1^2(\omega) + \varepsilon_2^2(\omega)]^{1/2} - \varepsilon_1(\omega)\}^{1/2} , \tag{18b}$$

$$\alpha(\omega) = \frac{2\omega k(\omega)}{c} , \tag{19}$$

$$R(\omega) = \frac{[n(\omega) - 1]^2 + k^2(\omega)}{[n(\omega) + 1]^2 + k^2(\omega)} , \tag{20}$$

where ε_1 and ε_2 are the real and imaginary part of the dielectric constant and $\hat{n}(\omega) = n(\omega) + ik(\omega)$ is the complex refractive index.

Following Genkin and Mednis,[19] $\chi_\pi(\omega)$ in the two-band model is given by

$$\chi_\pi(\omega) = \frac{4e^2}{(2\pi)^3} \int_{\mathrm{BZ}} d^3\mathbf{k} \left[\frac{|\mathbf{M}_{cv}(\mathbf{k})|^2}{\varepsilon_{cv}(\mathbf{k}) - \hbar\omega - i\hbar\Gamma} \right. \\ \left. + \frac{|\mathbf{M}_{cv}(\mathbf{k})|^2}{\varepsilon_{cv}(\mathbf{k}) + \hbar\omega + i\hbar\Gamma} \right] , \tag{21}$$

where e is the electronic charge, $\varepsilon_{cv}(\mathbf{k})$ is the energy difference between conduction and valence bands, BZ denotes the first Brillouin zone, and Γ is the broadening resulting both from lifetime effects and from the distribution of the transition energies originated by the different conjugation lengths present in the actual polymer. The factor 4 in Eq. (21) accounts for the presence of two chains, for each spin, in the unit cell.

This expression does not include the vibronic structure of the absorption spectrum originating from the strong electron-phonon interaction which has been observed in *cis*-polyacetylene[6–8] and in short polymers.[27] Although hidden in *trans*-polyacetylene by the distribution of the conjugation lengths, this effect is certainly present and rounds off the singularity at the absorption edge. Within the approximation of the displaced oscillator model, the electron-phonon interaction yields a number of vibronic replicas separated by the energy of the phonons coupled to the electronic transition and weighted, for the nth replica, by the intensity factor[8,28]

$$I_n = \frac{e^{-S} S^n}{n!} , \tag{22}$$

where S, the Huang-Rhys factor, is a measure of the displacement of the equilibrium position in the excited state relative to the ground state.

IV. RESULTS

A. Optical properties

The following values have been assumed for the evaluation of the optical properties: $\beta_1 = 2.5$ eV, $\beta_2 = 3.3$ eV, $\beta_\perp = 0.05$ eV, $1/\Gamma_\parallel = 6$ fs, $1/\Gamma_\perp = 70$ fs, $\hbar\omega_{\rm ph} = 0.15$ eV, $S = 0.68$,[29] $u_0 = 0.035$ Å (average value from Refs. 24 and 30), $a = 4.24$ Å, $b = 7.32$ Å, and $c = 2.48$ Å.[18] The value assumed for $\Gamma_\parallel$ reflects the distribution of the conjugation lengths which yields an inhomogeneous broadening of the absorption band of about 1 eV. The value adopted for the interchain hopping integral corresponds to a ratio $\beta_2/\beta_\perp \simeq 70$ which is similar to the ratio ($\simeq 85$) between the corresponding overlap integrals calculated using STO-3G atomic orbitals.[31] Our calculations show that for $\beta_\perp$ in the range 0.01–0.1 eV the overall perpendicular absorption is quite insensitive to the particular value of $\beta_\perp$ assumed. However, as it will be discussed in the following section, the value of $\beta_\perp$ strongly affects $\alpha_\perp^{3D}$ and therefore the pump anisotropy [Eq. (3)].

Since polyacetylene is oriented upon stretching, the chains in the plane perpendicular to the stretching direction are randomly oriented. In the comparison between the calculated and experimental optical properties, this fact has been taken into account by averaging the perpendicular absorption coefficient according to

$$\langle \alpha_\perp \rangle = \frac{1}{2\pi} \int_0^{2\pi} d\vartheta \, \alpha_\perp \cos^2\vartheta , \tag{23}$$

where ϑ is the angle between the polarization direction of the electric field and the axis of a particular chain.

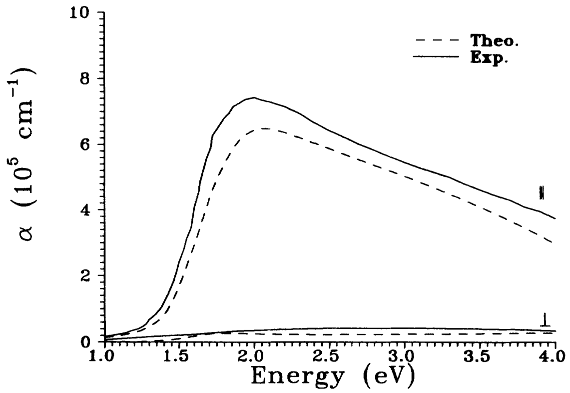

FIG. 4. Experimental (solid lines) and calculated (dashed lines) absorption coefficient polarized parallel and perpendicular to the chain axis. Calculated perpendicular data have been averaged according to Eq. (20). Experimental data are taken from Ref. 7.

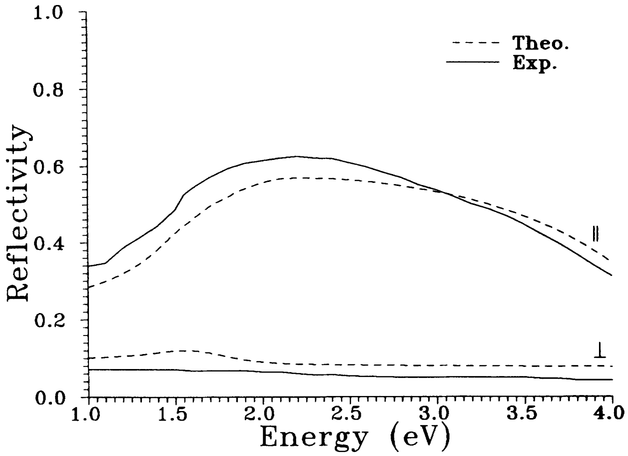

FIG. 5. Experimental (solid lines) and calculated (dashed lines) reflectivity for parallel and perpendicular polarization. Experimental data are taken from Ref. 7.

The absorption coefficient and reflectivity calculated for both polarizations are reported in Figs. 4 and 5 and compared with the experimental data obtained for highly oriented Durham *trans*-polyacetylene.[7] Even though minor discrepancies are observed, the frequency dependence of the optical properties can be considered satisfactory especially in consideration of the simplicity of the model. Figure 6 shows the details of the three contributions to $\alpha_\perp$. We notice that in Durham polyacetylene the main contribution to the perpendicular absorption comes from the perpendicular intrachain absorption ($\alpha_\perp^{1D}$) because the contribution related to the chain misalignment ($\alpha_\parallel/365$ for $\delta = 3°$)^2 is quite small. Figure 6 shows that the absorption maximum for $\alpha_\perp^{3D}$ peaks at lower energies than $\alpha_\parallel$. This is due to the fact that coupling between electronic transitions and C=C stretching phonons (that generates high-frequency phonon replicas of the joint density of states) does not occur for the interchain transitions.

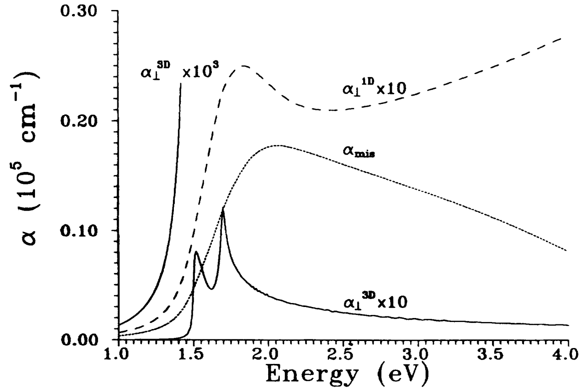

FIG. 6. Detail of the contributions to $\alpha_\perp$. $\alpha_\perp^{1D}$ (broken line); $\alpha_{\rm mis} = \alpha_\parallel/365$ (dotted line); $\alpha_\perp^{3D}$ (full line).

B. Photoconductive response

In this section we will discuss the anisotropy of the photoconductivity measured on samples of *trans*-$(CH)_x$ possessing fibrous morphology. Stretching of these samples results in a lower degree of orientation with respect to Durham $(CH)_x$ as shown by x-ray measurements which give a half width at half maximum chain orientation angle $\delta=7°$.

According to Eqs. (2a), (2b), and (3) the free-carrier generation anisotropy $(N_\perp/N_\parallel)$ depends on ξ and $\beta_\perp$. The carrier photogeneration efficiency, ξ, has been experimentally evaluated by Orenstein *et al.*[17] who have found that ξ drops by an order of magnitude from 2.2 eV down to 1.4 eV.

With the parameters used for optical properties an anisotropy of $\simeq 4.6$ at 2.34 eV and of 2.7 at 1.17 eV is obtained with a quantum efficiency of 1/400 at 2.34 eV and 1/1000 at 1.17 eV. The scaling of the quantum efficiency with the photon energy is consistent with the data reported in Ref. 17.

As already pointed out, the pump anisotropy is much more sensitive to $\alpha_\perp^{3D}$ and therefore to $\beta_\perp$ than the optical response function. The strong dependence of $N_\perp/N_\parallel$ on $\beta_\perp$ is reported in Figs. 7 (1.17 eV) and 8 (2.34 eV) for different values of the quantum efficiency.

Figures 7 and 8 show that below and above gap values can be reproduced with various pairs of $\beta_\perp$ and ξ. The particular couple $\beta_\perp,\xi$ selected determines the anisotropy in the gap region, which has not been yet fully experimentally investigated for fibrillar polyacetylene.

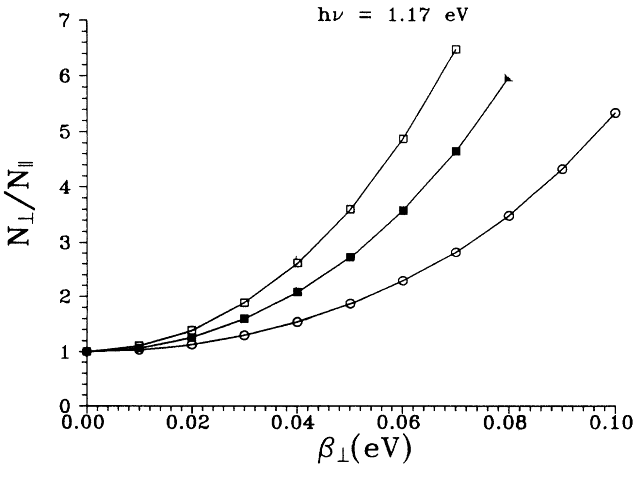

FIG. 7. Pump polarization anisotropy vs $\beta_\perp$ for below-gap (1.17 eV) excitation and for different values of ξ. □, $\xi=1/1500$; ■, $\xi=1/1000$; ○, $\xi=1/500$.

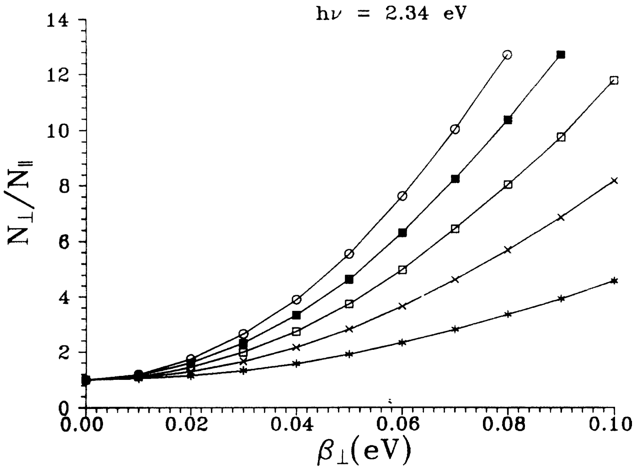

FIG. 8. Pump polarization anisotropy vs $\beta_\perp$ for above-gap (2.34 eV) excitation and for different values of ξ. ○, $\xi=1/500$; ■, $\xi=1/400$; □, $\xi=1/300$; ×, $\xi=1/200$; *, $\xi=1/100$.

Another important feature of the picosecond data (reported in Fig. 2) is the fact that the anisotropy is independent from the laser intensity for below-gap laser excitation, while it decreases with increasing laser intensity for excitation above the energy gap. There are two possible explanations for this behavior. At first sight the model here developed seems to be inconsistent with the dependence of the anisotropy on the laser intensity because both the transverse hopping integral and the quantum efficiency for carrier generation are clearly independent from the photon flux. However, heating effects generated by the laser pulse should be considered. In fact, for photon energies above the energy gap and polarized along the chain axis, the penetration depth into the sample is very small and a substantial amount of energy is deposited into a small volume for each pulse. If heat diffusion beyond the volume initially illuminated is neglected, the temperature increase following the pulse is given by

$$\Delta T=\frac{(1-R_\parallel)N\hbar\omega}{\rho c_p d_\parallel}\,, \tag{24}$$

where N is photon flux, c_p is the specific heat [1.43 J/gK (Ref. 32)], and ρ is the density of the polyacetylene sample (1.1 g/cm^3). Using Eq. (21) the difference in heating between the maximum (6×10^{15} photons/cm^2) and the minimum (3×10^{15} photons/cm^2) illumination is 137 K, which can be considered an upper value, because, within the duration of the pulse (25 ps), heat diffusion beyond the illuminated volume has been neglected. This ΔT is large enough to increase the hopping conduction, which has an activation energy of 0.043 eV,[4] so that the anisotropy decreases with the intensity as experimentally observed. The other explanation for the pump anisotropy can be found by assuming a bimolecular recombination of the carriers, which implies a photocurrent dependence on the inverse square root of the absorption coefficient

$$I_{\text{photocurrent}}=2ew(\xi I/\alpha\zeta)^{1/2}\mu[1-\exp(-\alpha t/2)]|\mathbf{E}|\,, \tag{25}$$

where w is the electrode width, μ the carrier mobility, $\mathbf{E}$ the static electric field, t the film thickness, I the laser intensity, and ζ the bimolecular recombination constant.

This kind of recombination becomes important when the concentration density is large. Bleier *et al.*[3] have ruled out the bimolecular decay path on the basis of the observation that the slow photocurrent component does not depend on the intensity. It is, however, not clear whether this argument is fully acceptable since the bimolecular recombination may affect only the early stages of the carrier dynamics and it is likely that the slow component of the photocurrent is controlled by recombination at impurities and defects in the sample.[33] Moreover in many experiments so far carried out only a small fraction of the electronic density is excited [typically 1/2000 (Ref. 31)]. In the present case the high photon flux (up to 6×10^{15} photons/cm^2) could give rise to some bimolecular recombination and therefore contribute to the observed pump anisotropy.

V. CONCLUSION

In this paper we have presented a model which is a rather straightforward application of the Su-Schrieffer-Heeger[30] Hamiltonian extended to include the zig-zag structure of the chain and the electronic coupling between chains. This model satisfactorily accounts for the observed optical properties, and since it implies a small but nonvanishing direct carrier separation on different chains ($\alpha_\perp^{3D}$), it predicts the observed anisotropy of the long-lived carriers, experimentally determined through photoconductivity and photoinduced absorption measurements.

The value of $\beta_\perp$ which has been used appears to be reasonable on the basis of the following considerations.

(i) $\beta_\perp/\beta_2$ scales with the ratio between the overlap integrals of the $2p\pi$ atomic orbitals of two nearest-neighbor carbon atoms in the chain and in different chains, as it should be according to the Mulliken approximation for the Hamiltonian matrix elements.[34]

(ii) The broadening effect of the 1D singularity introduced by the interchain coupling (of the order of $4\beta_\perp$) becomes comparable with the separation between the phonon replicas observed in the absorption spectrum of *cis*-polyacetylene.

We have already stressed that while optical anisotropies are quite insensitive to the value of $\beta_\perp$ (at least in the range 0.01–0.1 eV), the pump anisotropy of photoconductivity is critically dependent on the direct creation of charge carriers on different chains (through $\beta_\perp$) in addition to those arising from early hops (quantum efficiency ξ) to neighboring chains.

Although the present model, combined with the laser heating effects, accounts for the observed pump anisotropy both for below- and above-gap excitations and also for the intensity dependence of the anisotropy observed only for above-gap excitation, possible contributions from the bimolecular recombination, especially at high excitation densities, cannot be excluded.

ACKNOWLEDGMENTS

The authors are indebted to the Istituto di Chimica delle Macromolecole-CNR for the use of its facilities. We also thank Professor D. Baeriswyl and Dr. A. Piaggi for helpful discussions.

---

[1] R. Dorsinville, S. Krimchansky, R. R. Alfano, J. L. Birman, R. Tubino, and G. Dellepiane, Solid State Commun. **56**, 857 (1985).

[2] P. D. Townsend and R. H. Friend, Synth. Met. **17**, 361 (1987).

[3] H. Bleier, S. Roth, Y. Q. Shen, D. Schäfer-Siebert, and G. Leising, Phys. Rev. B **38**, 6031 (1988).

[4] A. D. Walser, R. Dorsinville, R. Tubino, and R. R. Alfano, Phys. Rev. B **43**, 7194 (1991).

[5] G. B. Blanchet, C. R. Fincher, T. C. Chung, and A. J. Heeger, Phys. Rev. Lett. **50**, 1938 (1983).

[6] D. Comoretto, R. Tubino, G. Dellepiane, G. F. Musso, A. Borghesi, A. Piaggi, and G. Lanzani, Phys. Rev. B **41**, 3534 (1990).

[7] G. Leising, Phys. Rev. B **38**, 10 313 (1988).

[8] D. Moses, A. Feldblum, E. Ehrenfreund, A. J. Heeger, T. C. Chung, and A. G. MacDiarmid, Phys. Rev. B **26**, 3361 (1982).

[9] P. M. Grant and I. P. Batra, Solid State Commun. **29**, 225 (1979).

[10] G. P. Agrawal, C. Cojan, and C. Flytzanis, Phys. Rev. Lett. **38**, 711 (1977).

[11] T. K. Lee and S. Kivelson, Phys. Rev. B **29**, 6687 (1984).

[12] P. L. Danielsen, J. Phys. C **19**, L741 (1986).

[13] Y. N. Gartstein and A. A. Zakhidov, J. Mol. Electron. **3**, 163 (1987).

[14] D. Baeriswyl and K. Maki, Phys. Rev. B **38**, 8135 (1988).

[15] K. Fesser, Phys. Rev. B **40**, 1962 (1989).

[16] X. Wang, D. K. Campbell, H. Q. Lin, and P. Vogl, Synth. Met. **41-43**, 3567 (1991).

[17] J. Orenstein, Z. Vardeny, G. L. Baker, G. Eagle, and S. Etemad, Phys. Rev. B **30**, 786 (1984).

[18] C. R. Fincher, C. E. Chen, A. J. Heeger, A. G. MacDiarmid, and J. B. Hastings, Phys. Rev. Lett. **48**, 100 (1982).

[19] V. N. Genkin and P. M. Mednis, Zh. Eksp. Teor. Fiz. **54**, 1137 (1968) [Sov. Phys. JETP **27**, 609 (1968)].

[20] C. Cojan, G. P. Agrawal, and C. Flytzanis, Phys. Rev. B **15**, 909 (1977).

[21] D. Comoretto, G. Dellepiane, G. F. Musso, R. Tubino, A. Walser, R. Dorsinville, and R. R. Alfano, Synth. Met. **41-43**, 3515 (1991).

[22] D. Comoretto, G. Dellepiane, G. F. Musso, R. Tubino, A. Walser, R. Dorsinville, and R. R. Alfano, in *Electronic Properties of Polymers,* edited by H. Kuzmany, M. Mehring, and S. Roth (Springer-Verlag, Berlin, 1992), Vol. 107, p. 68.

[23] F. Wooten, *Optical Properties of Solids* (Academic, New York, 1972).

[24] D. Baeriswyl, G. Harbeke, H. Kiess, E. Meier, and W. Meyer, Physica **117&118**, 617 (1983).

[25] R. G. Snyder, J. Mol. Spectrosc. **36**, 204 (1970); **36**, 222 (1970).

[26] R. H. Baughman and G. Moss, J. Chem. Phys. **77**, 6321 (1982).

[27] W. Siebrand and M. Z. Zgiersky, J. Chem. Phys. **71**, 3561 (1979).

[28] K. K. Rebane, *Impurity Spectra of Solids* (Plenum, New York, 1970).

[29] R. S. Cataliotti, G. Paliani, G. Dellepiane, S. Fuso, S. Destri, L. Piseri, and R. Tubino, J. Chem. Phys. **82**, 2223 (1985).

[30] W. P. Su, J. R. Schrieffer, and A. J. Heeger, Phys. Rev. B **22**, 2099 (1980).

[31] R. Dovesi (private communication).

[32] N. Mermillod, L. Zuppiroli, and B. François, J. Phys. (Paris) **41**, 1453 (1980).

[33] G. Kanner, Ph.D. thesis, University of Utah, 1991.

[34] P. M. Grant and I. P. Batra, Synth. Met. **1**, 193 (1979/80).